ACOUSTICAL TESTS OF MIDDLE-EAR AND COCHLEAR FUNCTION IN INFANTS AND ADULTS

Douglas H. Keefe
Boys Town National Research Hospital
555 North 30th Street
Omaha, Nebraska 68131

The peripheral processing of sound by the external ear, middle ear and cochlea precedes the neural encoding of sound. The external ear collects sound power that is transmitted and reflected within the ear canal, absorbed by the middle ear, and transmitted as a coupled mechanical-fluid wave motion within the cochlea. The cochlea analyzes the time-varying frequency components of the incident sound and converts them into a spatial-temporal distribution of neural spikes in the fibers of the auditory nerve. This encoded signal is subsequently analyzed by the brain through detection and classification processes, which enables the human listener to construct a perceptual and cognitive map of the auditory world.

"Absorbed sound power can control for ear-canal and middle-ear sources of variability across frequency in physiological, behavioral and clinical measurements of auditory function."

The relative efficiency through which sound is transmitted from the external field of the listener to the cochlea varies with age, and thereby constrains the maturation of hearing. An important practical goal of measuring acoustical responses within the ear canal is to identify the presence of, and quantify the effects of, any dysfunction in the acoustical and mechanical pathway of sound transmission. Such information is clinically important in screening and diagnosing hearing loss, which would negatively affect speech perception and music perception. Of particular note is the growth in the last couple of decades in universal newborn hearing screening programs to identify hearing loss. This article describes how acoustical measurements in the ear canal in response to sound are used to study and clinically assess hearing in children and adults.

A brief tour of ear anatomy and physiology

The external ear includes the visible structures on the side of the head such as the irregular concave surface of the pinna and the concha cavity, from which the ear canal entrance leads to the eardrum via a curved canal with a length of about 2.5 cm in the adult. The middle ear includes the eardrum, a space bounding the interior surface of the eardrum called the tympanic cavity, and three small bones known as ossicles that couple displacements of the eardrum to a displacement of what is termed the oval window of the inner ear. The tympanic cavity is vented to the nasal cavity via the Eustachian tube, which acts to equalize air pressure across the eardrum. The ossicular chain includes the malleus, which is connected to the eardrum, incus and stapes, which is attached to the oval window. A set of ligaments support the ossicles within the cavity. A stapedius muscle attached to the stapes can alter the stiffness of an annular ligament that couples the stapes footplate to the oval window, which can thereby alter the amount of sound-induced mechanical energy transmitted into the cochlea. From an acoustical perspective in normal hearing, the functional role of the middle ear is to transmit acoustical sound energy from the external ear into a coupled mechanical-fluid motion within the inner ear, and otherwise overcome the large impedance mismatch between air and fluid.

The cochlea, which is part of the inner ear, is a bony spiral shell that contains three fluid-filled compartments in which are found the cellular structures of the cochlear partition. The fluids within scala vestibuli and scala tympani compartments are continuously joined at the extreme apical end of the cochlear spiral. The cochlea is coupled at its base to the tympanic cavity of the middle ear via the oval window, whose motion drives a motion of the nearly incompressible fluid in scala vestibuli, and the round window, which moves in response to a motion of fluid in scala tympani. An inward motion of the oval window displaces the cochlear fluid and generates an outward motion of the round window. A pressure difference results across the flexible cochlear partition, which moves in response to this time-dependent force. This partition includes the basilar membrane on which is placed the organ of Corti. The cellular structures on the organ of Corti are the most mechanically sensitive in the human body, and form a critical part of our ability to hear over a ten-octave range of frequency and 120-dB range of sound pressure level.

Through a remarkable series of experiments in the mid-20th century using partially intact cochleae of human cadavers, Békésy (1989) discovered that sound produced an activation pattern of transverse wave displacement of the basilar membrane that had its maximum at high frequencies close to the base and at low frequencies close to the apex. This frequency-to-place (tonotopic) encoding of auditory signals at the cochlear level is extensively replicated throughout the brain structures that process auditory information. Basilar-membrane motion displaces the organ of Corti and induces fluid motion in scala media to displace the cilia of the inner hair cells. This ciliary motion gates an electrical current flow into the inner hair cell, which controls spike generation in afferent fibers of the VIIIth (auditory) nerve at the base of the hair cell. The resulting spike trains are transmitted to the brainstem.

Basilar membrane motion in responses to pure-tone

stimulation has a compressive nonlinearity (Rhode, 1971), which results in much sharper mechanical tuning at sound levels close to threshold and broader tuning at higher sound levels. The pure-tone excitation pattern of the traveling wave along the basilar membrane has a larger relative amplitude at lower sound levels at locations just basal to its tonotopic place than its relative amplitude at higher sound levels (i.e., this is the region of compressively nonlinear growth in amplitude). The outer hair cells in the organ of Corti act as a saturating feedback amplifier to achieving this sharper tuning at sound levels near threshold. From the perspective of identifying ears with hearing loss, damage to outer or inner hair cells or reductions in the electrical potential across the hair cells can lead to sensorineural hearing loss.

Intermodulation distortion and two-tone suppression effects are observed when two or more pure tones are presented simultaneously. These processes are intimately related to the compressive nonlinearity of basilar-membrane mechanics. In the 19th century, Helmholtz described an auditory theory for the combination tones heard out by listeners when two pure tones are presented simultaneously; detailed psychophysical data and models are available (Goldstein, 1967). A correlate to such distortion tones was found in single-fiber recordings from the auditory nerve (Goldstein and Kiang, 1968), and in recordings of basilar-membrane displacement (Nuttall *et al.*, 1990; Robles *et al.*, 1990). In single-fiber recordings from the auditory nerve in monkey (Nomoto *et al.*, 1964) and cat (Kiang *et al.*, 1965, Sachs and Kiang, 1967), the presence of one pure tone influenced the neural firing rate associated with another pure tone at a higher or lower frequency. This two-tone suppression effect was also found in mechanical recordings on the basilar membrane (Rhode, 1977), which supports the modern view that sharp mechanical tuning is responsible for sharp neural tuning. Such suppression effects (and other effects at more central levels in the auditory system) improve a listener's ability to perceive speech in noise. For a pure tone (called the probe tone) presented at a low to moderate level, a suppression tuning curve is constructed by measuring the sound pressure level (SPL) needed of a second suppressor tone to reduce the response to the probe tone by a reference amount at a set of suppressor frequencies above and below the probe frequency. A suppression tuning curve is a plot of this critical SPL versus suppressor frequency.

The acoustic reflex forms a feedback pathway connecting middle-ear, cochlear and neural levels of auditory function. This reflex triggers an action of the stapedius muscle to stiffen the ossicular chain of the middle ear (at least at low frequencies) in response to the presentation of a relatively high-level sound. Neural signals generated in response to sound ascend via the VIIIth nerve and are processed centrally; neural efferents descend via the VIIth (facial) nerve to activate the stapedius muscle, which influences middle-ear transmission.

One task of an aural acoustical test in the clinical setting is to reveal potential sources of dysfunction within the middle ear, cochlea and neural processes that affect the acoustical response measured in the ear canal. The next section summarizes past approaches to middle-ear testing.

Middle-ear tests: Acoustic impedance and admittance tympanometry

While acoustical impedance measurements of the ear were initially reported in the late 1920's and 1930's, Metz (1946) was the first to obtain clinically significant results in measuring acoustical impedance in substantial groups of ears with normal function and ears with middle-ear disease. The impedance was measured using an acoustic bridge technique at ambient pressure in the ear canal. The bridge had a sound source symmetrically placed in the middle of a cylindrical tube, one end of which was coupled into the ear canal in a leak-free manner. Its opposite end was terminated in a set of acoustic couplers of adjustable, but known dimensions. The sound source generated an outgoing sinusoidal sound wave of equal amplitude but opposite phase in the two tubes. The observer listened using a stethoscope via a tube coupled to each side of the tube near its middle with a Y-tube connection, and adjusted the coupler dimensions until a minimum audible sound was detected. This null represented the frequency-specific condition in which the impedances on both sides were equal. The acoustic bridge had to be re-adjusted at other test frequencies, and the acoustic effect of the volume of air in the part of the ear canal between the tube end and the eardrum was unaccounted for. Metz also used the acoustic bridge to measure the acoustic reflex response in terms of a shift in the acoustic impedance of the ear. The acoustic reflex threshold is the lowest level activator that elicits a detectable shift in the acoustic impedance.

An innovation that led to improved clinical utility was the measurement of acoustic impedance over a range of ear-canal air pressures in a test called tympanometry (Terkildsen and Thomsen, 1959). This pressurization differentially affected the mobility of the eardrum as assessed using a pure tone. Tympanometers to measure aural acoustic admittance (i.e., the inverse of impedance) at a single frequency close to 226 Hz use a pump to control air pressure and a probe with a leak-free insertion into the ear canal. Tympanometers were in widespread clinical use by the 1970s and are the dominant clinical testing device of middle-ear function used today.

Acoustic admittance is useful in a measurement in which the acoustic pressure in the ear canal is the input variable and the volume velocity swept out by the eardrum is the output variable. In an ear with normal function, the resulting admittance magnitude tympanogram is plotted as a function of excess air pressure within the ear canal. This pressure is controlled by the pump over a range of approximately 2-3% deviation from atmospheric pressure (e.g., -300 to +200 daPa). The admittance magnitude at the probe has a single-peaked shape that can be used to measure admittance magnitude at the eardrum under certain assumptions. These assumptions, which are of limited validity, are: the eardrum is immobile at the most positive or most negative "tail" pressure, the cross-sectional area does not vary with air pressure, and acoustic wave effects in the ear canal are negligible (Shanks and Lilly, 1981). If the eardrum is immobile at the tail pressures, then the probe admittance equals the admittance of the enclosed volume of air, which acts at low frequencies as a compliance.

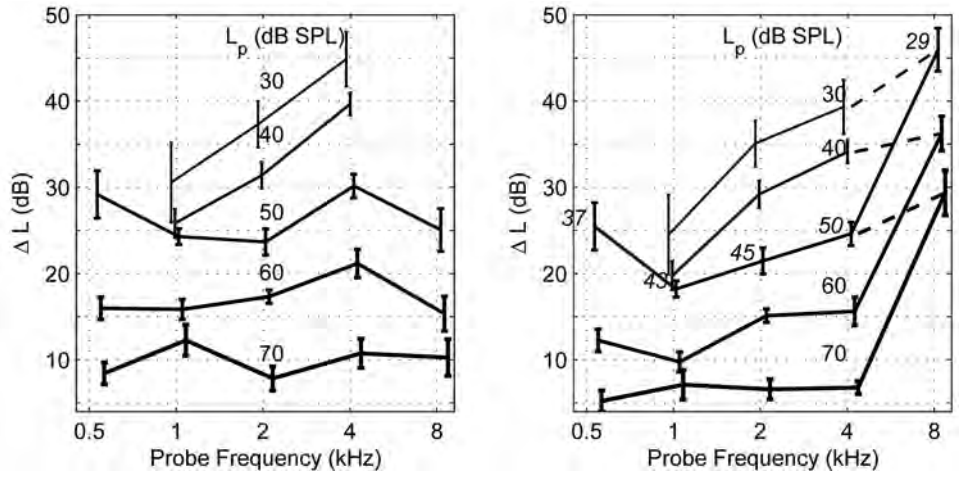

Fig. 1. Left: Mean ± SE of the tip-to-tail Sound Pressure Level (SPL) difference of the stimulus frequency otoacoustic emission (SFOAE) suppression tuning curve at each probe frequency. L_p specifies SPL in the column for each equal-SPL contour (solid curves). Right: Mean ± SE of the tip-to-tail power-level difference of the SFOAE sound transmission curve (STC) at each probe frequency. L_p specifies SPL in the column for each equal-SPL contour (solid curves). The absorbed power level is row-specified for the contour at 50-dB SPL; e.g., at 4 kHz on this contour, the SPL is 50 dB and absorbed power level is 50 dB. The dashed lines between 4 and 8 kHz connect the tip-to-tail power level differences at approximately equal absorbed power levels of (± 1 ± dB). Curves are slightly displaced horizontally to improve clarity. [This figure was originally published in Keefe and Schairer (2011)]

It follows that the equivalent admittance at the eardrum is calculated at low frequencies by subtracting this volumetric admittance from the probe admittance. Higher test frequencies up to 1 kHz have been recommended, especially in testing infant middle ears. This combination of single-frequency admittance tympanometry and acoustic reflex measurements is the current clinical standard to assess middle-ear function. Acoustic reflex threshold and supra-threshold responses are usually measured based on the admittance shift detected at a single frequency (226 Hz in adults). Such reflex measurements are helpful in differentiating middle-ear and cochlear dysfunction, and VIIIth- and VIIth-nerve pathologies.

Cochlear tests using otoacoustic emissions

Compressive nonlinearities in cochlear mechanics were studied in mammalian and other non-human ears by increasingly detailed measurements in animal models, yet such invasive testing is impossible to perform in human patients for ethical reasons. A basic experiment in acoustics is to measure the impulse response of a system. Kemp (1978) presented a brief duration impulse sound into the ear canal and used a sensitive miniature microphone to detect its response. Whereas multiple reflections in the ear canal between the probe and eardrum have a duration of several milliseconds (ms), Kemp detected signal energy with delays as long as 12 ms. These so-called click-evoked (CE) otoacoustic emissions (OAEs) were found to be of cochlear origin, and associated with reflections from the cochlear traveling wave due to localized mechanical impedance discontinuities. Other types of OAEs were measured using other stimulus types. A stimulus-frequency (SF) OAE was measured at a single frequency by taking account of the compressive nonlinearity of cochlear mechanics (Kemp, 1979a), or by suppressing the stimulus-frequency response through the use of a second tone. Distortion-product (DP) OAEs were measured as a correlate to intermodulation distortion in cochlear mechanics using two pure tones of frequencies f1 and f2>f1 (Kemp, 1979b), with the most commonly measured DPOAE at 2f1-f2. Typical clinical tests use f2 close to 1.2 f1. Distortion is maximal at the f2 tonotopic place where the cochlear excitation patterns of f1 and f2 have the largest spatial overlap.

OAE measurements do not directly probe the nonlinear mechanics of the cochlear partition inasmuch as sound stimuli are generated and responses are measured in the ear canal rather than the cochlear partition. Notwithstanding this fact, OAEs can be detected non-invasively through acoustical measurements in the ear canal, and this has led to their widespread use in clinical testing since the 1990s. Evoked OAEs assess the feedback role of outer hair cells in achieving sharp tuning. Most current clinical OAE testing is performed using either CEOAEs or DPOAEs. OAE measurements can assess cochlear function from frequencies as low as about 0.5 kHz in adults and 1.5 kHz in infants, and as high as 16-20 kHz. Lower-frequency OAE measurements are limited by internal physiological noise (especially in infants) and reduced forward stimulus transmission through the middle ear. Clinical OAE testing is often confined to the 1-4 kHz range or 1.5-4 kHz in infants.

By analogy with two-tone suppression measured mechanically and neutrally in mammalian ears, two-tone suppression is measured in human ears by suppressing an OAE response using an additional suppressor tone. For the case of a SFOAE measured at a fixed probe frequency, fp, and a fixed probe level, Lp, a suppressor tone is added at a suppressor frequency, fs, and its suppressor level, Ls, is varied to achieve a criterion change in the SFOAE level at fp (Brass and Kemp, 1993). A suppressor frequency close to fp (i.e., within a few percent) at the "tip" of the tuning curve is influenced by about the same compressive nonlinearity as fp. A suppressor frequency an octave below fp at the low-frequency "tail" of the tuning curve has its peak response at a more apical location on the basilar membrane than the tonotopic peak region of fp where the SFOAE is generated. The entire excitation

pattern of fp on the basilar membrane is basal to the active region of amplification of the excitation pattern at fs so that the basilar-membrane response at fp is linearly suppressed by growth in the tone at fs in the tail region. That is, a 1-dB increase in suppressor level produces greater reduction in the OAE level at the tail frequency than the tip frequency. The difference in suppressor SPL needed to produce the same change in SFOAE level is called the tip-to-tail pressure-level difference, and is plotted in the left panel of Fig. 1 as a function of fp. Each curve shows the tip-to-tail level measured using a single probe level (Lp) (Keefe *et al.*, 2008).

The overall reduction with increasing Lp in the tip-to-tail differences across fp is consistent with the action of a compressive nonlinearity: cochlear amplification is increased at lower stimulus levels. At low and moderate Lp levels (30-60 dB SPL), the tip-to-tail difference between 1-4 kHz increases with increasing frequency, which suggests increased cochlear amplification, and thus sharper tuning, at high frequencies than low. This is consistent with increased sharpness of tuning in the human cochlea as frequency increases (Shera *et al.*, 2010). However, the tip-to-tail difference at 8 kHz was less than that at 4 kHz, which would appear to suggest a reduced cochlear amplification and broader tuning.

A suppression tuning curve can also be measured using DPOAE measurements (Brown and Kemp, 1984). The unsuppressed DPOAE is generated using a pair of tones with fixed frequencies (f1 and f2 $\approx$ $_{1.2}$ f1) and fixed levels, and then an additional tone is introduced in the ear canal to suppress the DPOAE level at 2f1-f2 by a criterion amount. Extensive measurements of DPOAE suppression tuning curves in adults across frequency (0.5-8 kHz) and level (50-dB range) are reported in Gorga *et al.* (2011). Maturation of DPOAE suppression tuning curves was studied in infants relative to adults (Abdala, 2001) with the largest maturational differences found at a f2 of 6 kHz. DPOAE suppression tuning curves at 6 kHz were more sharply tuned in ears of full-term infants and six-month-olds than in adults, as illustrated in Fig. 2.

While suppression of SFOAEs and DPOAEs primarily involves the action of cochlear nonlinearities, the stimuli presented in the ear canal to evoke the OAEs are transmitted in the forward direction through the middle ear to the cochlea, and OAE responses generated within the cochlear are transmitted in the reverse direction through the middle ear to the ear canal. Thus, an understanding of the high-frequency behavior of SFOAE suppression and the maturational differences in DPOAE suppression might depend on these transmission pathways.

Wideband tests of middle-ear function

While OAE testing is available over several octaves of frequencies important to speech perception, the restriction of compensated admittance tympanometry to 226 Hz is a serious limitation. This has most impact for measurements in infant ears, for which 226-Hz tympanometry is inaccurate. The presence of significant acoustical standing waves above 0.7 kHz in the adult ear canal limits the ability to interpret acoustic admittance measurements at higher frequencies,

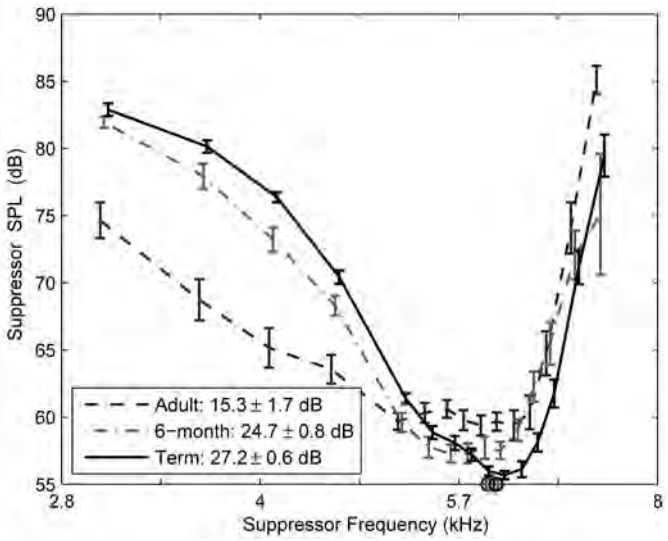

Fig. 2. Distortion product otoacoustic emission (DPOAE) tuning curve based on mean suppressor sound pressure level (SPL) (±1 standard error) for f2 frequency of 6 kHz. Legend specifies the age group and the tip-to-tail pressure level for that group. Circles at f2 of 6 kHz represent the stimulus level L2 of 55 dB SPL. Plots are slightly displaced horizontally to improve clarity. [This figure originally published in Keefe and Abdala (2011)]

because the admittance measured at the probe tip cannot be transformed to the eardrum admittance without further measurements and modeling.

A promising approach to clinical testing would be to use wideband testing for both middle-ear and cochlear responses. This led researchers to consider the use of aural acoustic reflectance for middle-ear testing. A one-dimensional sound field in an idealized long tube of constant cross-sectional area is a superposition of forward and reverse traveling waves, with forward denoting the direction from the sound source towards some discontinuity. The ratio of the reverse pressure to forward pressure at the discontinuity is the acoustic pressure reflectance, $R(f)$. Its squared magnitude $|R(f)|^2$ is energy reflectance, i.e., the ratio of reflected to incident energy from a transient sound. In the limit of negligible energy losses within the tube, energy reflectance is constant along the tube. The cross-sectional area of the ear canal varies sufficiently slowly and its length is sufficiently short that the integrated viscothermal losses at the canal walls are small in the frequency range of interest. Thus, the energy reflectance measured at interior locations within the ear canal at ambient air pressure can be used as a high-frequency measurement (above 1 kHz) of energy reflectance at the eardrum (Stinson *et al.*, 1982; Hudde, 1983).

Because earlier procedures were not intended for routine clinical use, especially in infant ears, an acoustic reflectance measurement system for human ears was designed to operate over a wideband frequency range using clinical eartips. Reflectance measurements were obtained in ear canals of adults and infants as young as 1 month from 0.125 to 10.7 kHz (Keefe *et al.*, 1993). This and other adult reflectance measurements (Voss and Allen, 1994) straddled the low frequencies used in clinical tympanometry and the high frequencies used in OAEs. An aural acoustic transfer function well suited to clinical use is acoustic absorbance, which is the

ratio of the sound energy absorbed by the ear to the incident energy from a transient sound. The absorbance, which is equal to $1-|R(f)|^2$, is insensitive to probe position within the ear canal. As shown in Fig. 3 for ears of adults and children from full-term infants to age 6 months with normal auditory function (Keefe and Abdala, 2007), the median absorbance in each age group varies from 1, when all energy is absorbed by the middle ear, down to 0, when no energy is absorbed by the middle ear (i.e., when all energy is reflected back into the ear canal). The middle ear is most efficient at absorbing sound energy at frequencies between 2 and 4 kHz except for full-term infants showing excessive absorbance at low frequencies. Because the ear-canal wall is not yet fully ossified in full-term infants, the ear-canal diameter can increase as much as 70% at air pressures in the tympanometric range (Holte *et al.*, 1991). Increased absorbance at lower frequencies in young infants is likely due to increased viscoelastic wall mobility (Keefe *et al.*, 1993, Qi *et al.*, 2006).

Clinical acoustical testing using insert earphones depends on sound transmission through the ear canal and middle ear as terminated by the input impedance of the cochlea. Under normal listening conditions, sound power is collected by the larger structures of the external pinna, transmitted through the ear canal, absorbed by the middle ear, and transmitted into the cochlea. A diffuse-field absorption cross-section A_D with units of area (Rosowski *et al.*, 1988; Shaw, 1988) quantifies the ability of the ear to absorb sound power from a reverberant sound field in a room. This measure is obtained by averaging over all directional attributes of the sound source and listener. (A listener's ability to localize a sound source depends critically on these monaural directional attributes, and this ability is greatly enhanced by the fact that the listener hears binaurally—i.e., based on input from each of two ears).

The A_D measured in Keefe *et al.* (1994) varied with frequency with a maximum value of about 800 mm^2 for an adult ear, but only about 63 mm^2 for the ear of a six-month-old. This age variation is controlled by post-natal growth of external ear structures (pinna, concha, ear canal) and maturation of middle-ear mechanics. The power efficiency of the overall adult human ear is exemplified by the maximum A_D of 800 mm^2 from diffuse sound field to ear canal, 50 mm^2 for the ear-canal area, and 3.2 mm^2 at the oval window of the cochlea, an overall areal level difference of 24 dB. An estimate of the "area" of external pinna comes from Teranishi and Shaw (1968), who constructed an external-ear model based on acoustical measurements in real ears and models. Their model was composed of a smaller cylinder (i.e., a "concha") embedded in a rectangular-shaped "pinna" of area 2160 mm^2 (i.e., 30 mm wide and 72 mm long). This model matched resonance frequencies for various angles of incident sound up to 7 kHz. This area is larger than the maximum A_D of 800 mm^2, as would be expected because much of the sound power incident on the ear is reflected.

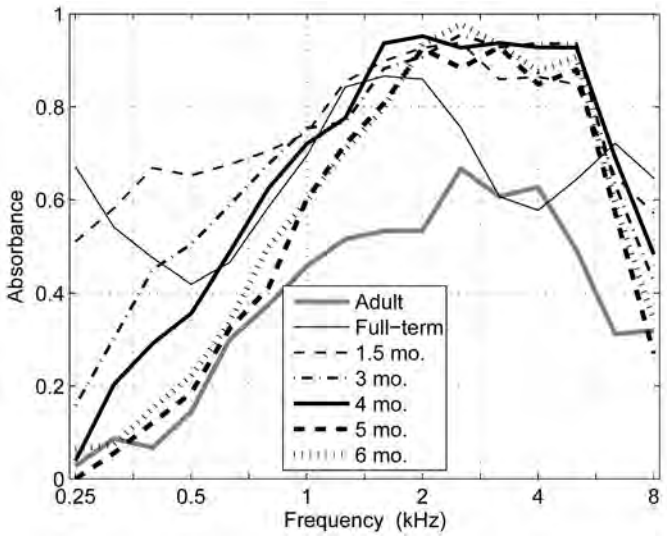

Fig. 3. Measured absorbance at ambient pressure in the ear canal is plotted versus frequency for groups of full-term infant ears, infant ears in age groups from 1.5 to 6 months, and adult ears.

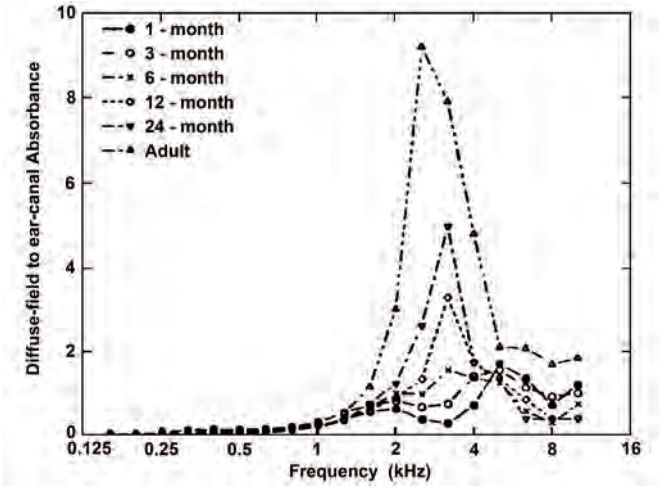

Fig. 4. Diffuse-field to ear-canal absorbance is plotted versus frequency for groups of infants at age 1 to 24 months, and adults. [This figure originally published in Keefe et al. (1994)]

The dimensionless ratio of the area A_D to the cross-sectional area of the ear canal at each age is plotted as a diffuse-field to ear-canal absorbance in Fig. 4. The diffuse-field to ear-canal absorbance is always positive and exceeds 1 for each age group, with a maximum of 9 for adults at about 2.7 kHz and 1.6 for six-month-olds at about 3.2 kHz. This is in direct contrast to the ear-canal absorbance plots in Fig. 3 that never exceed 1. This difference between the pair of absorbances illustrates the additional sound power collected by the pinna and other external-ear structures that are more distal to the location in the clinical test of an eartip within the ear canal. The acoustics is more complicated because the spatial sound field is inherently three-dimensional near the pinna as influenced by head and body diffraction, but is approximately one-dimensional in the interior of the ear canal a few mm from its entrance at its junction to the concha and from its termination at the eardrum. In practice, clinical measurements are considerably simplified by placing the sound source within the ear canal (although headphone presentation of sound is also used in audiological testing).

A wideband tympanometry test was developed based on reflectance measurements (Keefe and Levi, 1996). Based on audiologists' experience using 226-Hz admittance tympa-

nometry in which an adult ear with normal function has a single-peaked tympanogram, it is helpful to define a wideband tympanogram in terms of absorbance. This is because an absorbance tympanogram also has a single-peaked shape in an ear with normal function. The top panel of Fig. 5 shows an absorbance tympanogram recorded in an adult ear with normal middle-ear function as a joint function of frequency. Based on a transition frequency of 2 kHz, this tympanogram is reduced to a pair of low pass- (LP, in solid line) and high pass- (HP, in dashed line) averaged absorbance tympanograms versus air pressure on the bottom left panel. The tympanometric peak pressure (TPP) of -20 daPa is the peak pressure of the LP-averaged tympanogram; this peak is evident in the top panel. Its tympanometric width (TW) of 124 daPa is calculated as the range of pressures over which the absorbance exceeds one-half of its peak value (of 0.46). The HP-averaged absorbance tympanogram (lower left panel, dashed line), has a pressure asymmetry: the absorbance at positive pressures (compressing the ossicular chain) is larger than at negative pressures. The grey band and the pair of dotted lines on each lower panel show the 80th and 90th percentiles of normal response from Liu *et al.* (2008). The bottom right panel shows the absorbance at TPP as a function of frequency (solid line); the corresponding dashed line is the absorbance measured at ambient pressure (this is a single-ear example of the average adult absorbance in Fig. 3). The absorbance plots at ambient pressure and at TPP are similar in this ear because the TPP was close to ambient (0 daPa). However, these would, in general, differ in an ear with TPP different from ambient pressure and such information may be clinically relevant—negative TPPs are common in middle-ear disorders in children. Wideband absorbance tympanometry combines information found in single-frequency admittance tympanometry with information found at higher frequencies in an ambient absorbance response. Research is underway to assess the accuracy of these wideband tests in screening and diagnosing middle-ear dysfunction.

The use of a wideband probe stimulus allows for acoustic reflex measurements at lower activator levels than conventional clinical devices using a probe stimulus at a single frequency (Feeney and Keefe, 1999). This is mainly because a shift is easier to detect when measured over a wide frequency range than at a single frequency. A wideband reflex test may improve the safety of clinical reflex testing because acoustic-reflex decay measurements cause permanent hearing loss in some ears due to excessively high activator levels (Hunter *et al.*, 1999).

Absorbed sound power

Although sound levels are typically specified in hearing research in terms of acoustic pressure, the presence of acoustical standing waves in the ear canal leads to complications at high frequencies. An ear-canal sound source can also be specified in terms of the sound power absorbed by the ear

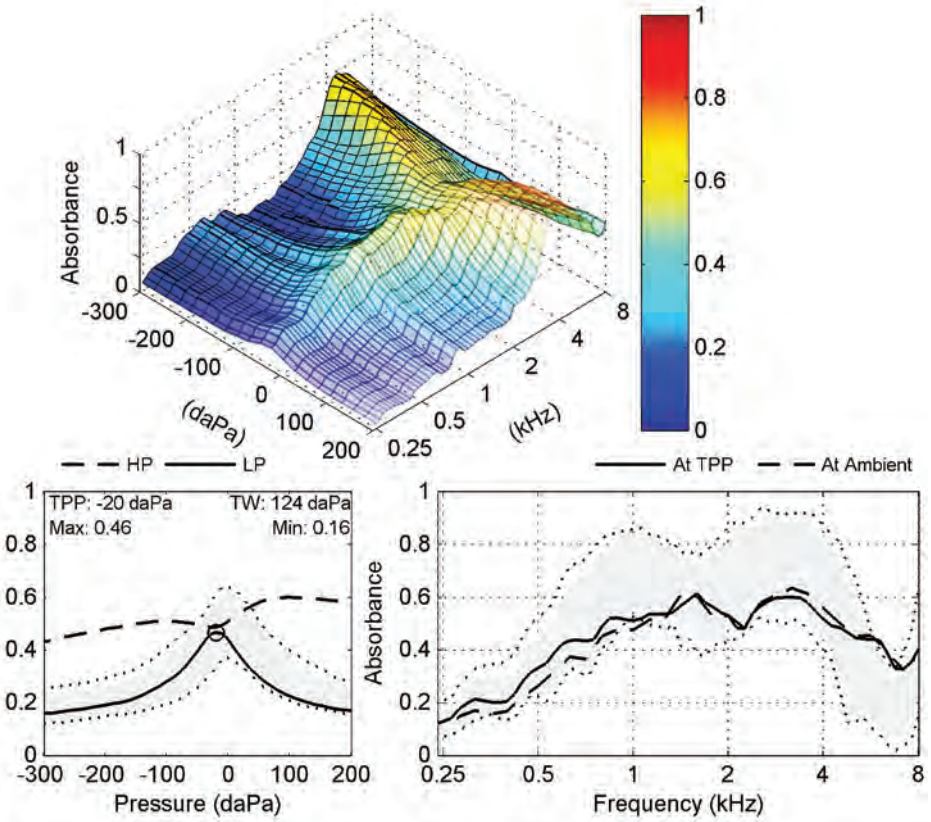

Fig. 5. Measured wideband absorbance tympanogram in adult ear versus frequency and tympanometric pressure (top). Low pass (LP, solid line) and high pass (HP, dashed line) averaged absorbance tympanograms are plotted versus pressure (bottom left). This panel shows the tympanometric peak pressure (TPP), tympanometric width (TW), minimum (Min) and maximum (Max) values of the LP-averaged absorbance tympanogram. Absorbance at the TPP is plotted versus frequency (solid line) along with the separate measurement of absorbance at ambient pressure (dashed line) (bottom right). The plots in the bottom panel also show 80th and 90th percentiles of adult-ear responses with normal middle-ear function (gray fill and dotted line, respectively).

as long as an acoustic transfer function such as admittance is measured. Calibration based on absorbed sound power is an attractive alternative to that based on sound pressure level for a wide variety of aural acoustical measurements.

For a mean-squared pressure magnitude $|p(f)|^2$ and acoustic conductance $G(f)$ at frequency, f, the absorbed sound power is $W(f)=G(f)|p(f)|^2$. The conductance level $L_G=10\log_{10}G$ in a normal adult ear increases with a slope of about 4.5 dB per octave from low frequencies up to 4.5 kHz, and then steeply decreases by about 20 dB up to 8 kHz. A conductance measurement makes it possible to construct a sound stimulus with constant absorbed sound power across frequency in a particular ear. Except for the case of the infant ear canal with additional power loss at low frequencies, nearly all the sound power is absorbed by the middle ear.

SFOAE suppression tuning curves in adult ears were introduced earlier as a measure of cochlear nonlinearity at suppressor frequencies around a probe frequency. SFOAE suppression can also be interpreted in terms of the sound power absorbed at both the probe and suppressor frequencies (Keefe and Schairer, 2011). The originally unsuppressed SFOAE response was recorded at a fixed probe level Lp as indicated by the 30 to 70 dB SPL values shown on each equal-SPL curve on the left panel of Fig. 1. Based on measurements of acoustic conductance, L_G was normalized to 0 dB for G=1 1 mmho (this commonly used audiological unit is mmho=10^{-8}m^4·s/kg). The resulting absorbed power level $L_a=10\log_{10}W=L_G+SPL$ varied with probe frequency as indicated by the values along the 50-dB contour in the right panel of Fig. 1. e.g., L_a was 43 dB at 1 kHz, 50 dB at 4 kHz, but only 29 dB at 8 kHz, with similar L_G-related offsets on other contours. The tip-to-tail pressure-level difference on the ordinate of the left panel of Fig. 1 was converted to a tip-to-tail power-level difference shown in the right panel by converting the SPL at the tip and tail into L_a. The lower dashed line between the data at 4 and 8 kHz on the right panel connects the tip-to-tail power-level difference at a probe L_a of 50 dB at 4 kHz to that at a L_a of 49 dB at 8 kHz; i.e., this pair of frequencies had equal absorbed power level to within 1 dB even though their ear-canal SPL differed by 20 dB. Based on these transformations, the tip-to-tail power-level difference was larger at 8 kHz than at 4 kHz. This is consistent with the theory that human cochlear tuning is sharper at high frequencies (Shera *et al.*, 2010). A similar transformation of the DPOAE suppression tuning curve from SPL to absorbed sound power level was applied to the infant and adult responses in Fig. 2. When the SPLs of the stimuli used to generate and suppress the DPOAE were used with age-dependent conductance measurements to calculate absorbed power, the resulting power-based suppression tuning curves shown in Fig. 6 were nearly identical for full-term infants, six-month-olds and adults (Keefe and Abdala, 2011).

The example of SFOAE suppression shows how an in-the-ear calibration based on absorbed sound power has advantages over ear-canal pressure calibration in interpreting cochlear-generated responses at high frequencies. The example of DPOAE suppression supports the theory that the maturation of DPOAEs can be accounted for by maturation of

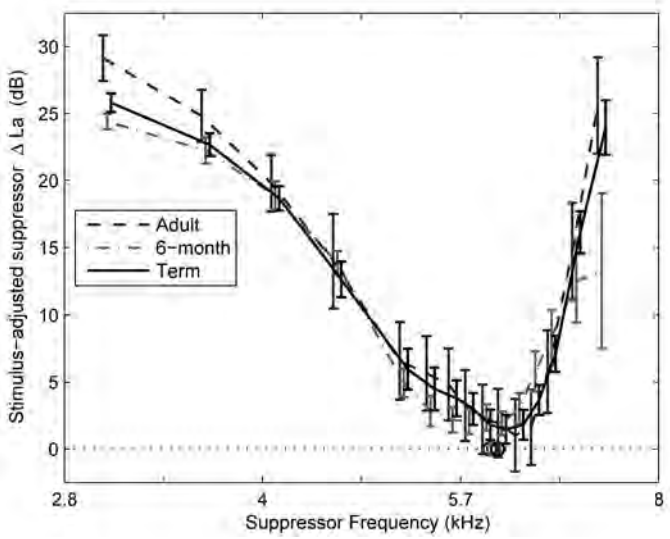

Fig. 6. Distortion product otoacoustic emission (DPOAE) tuning curve based on ΔL_a (± 1 standard error), the difference in L_a and absorbed power level of the stimulus based on L2 and the mean conductance level at f1 and f2. Circles at f2 of 6 kHz and 0 dB show the normalization of each tuning curve to the absorbed DPOAE stimulus power. Plots are slightly displaced to improve clarity. [This figure originally published in Keefe and Abdala (2011)]

ear-canal and middle-ear function in an infant with mature cochlear mechanics. This and alternative theories of possible cochlear sources of maturation are explored in Abdala and Keefe (2012). An in-the-ear calibration based on absorbed sound power can control for ear-canal and middle-ear sources of variability across frequency in other physiological, behavioral and clinical measurements of auditory function.

Newborn hearing screening (NHS) to identify ears with hearing loss

Between 2000 and 2009, the percentage of newborn infants screened for hearing loss in the U.S. increased from 38% to 97%. The Joint Committee on Infant Hearing (JCIH) mandates screening infants at no later than 1 month of age, because "unidentified hearing loss at birth can adversely affect speech and language development as well as academic achievement and social-emotional development" (JCIH, 2007). The large scope of the program can be appreciated by the fact that over 3.9 million infants were screened in 2009 in the U.S., and NHS programs are implemented in countries around the world. Objective NHS tests include either or both of an OAE and auditory brainstem response (ABR) for newborns in well-baby nurseries, or an ABR for infants in a neonatal intensive care unit (NICU) because of increased risk for a permanent hearing loss.

An ABR test is a peripheral neurodiagnostic test for cochlear disease and VIIIth nerve and brainstem disease. Using electrodes attached to the scalp and sound stimulation in the ear canal, an ABR is composed of a voltage signal detected within the initial 15 ms of stimulus onset from a brief sound presented in the ear canal, as reviewed by Don and Kwong (2009). An ABR test is more time consuming and costly than an OAE test. Nevertheless, the ABR test is recommended by JCIH for NICU babies because they are at higher risk for sensorineural hearing loss, and because neu-

ral conduction disorders or auditory neuropathy/dyssynchrony in the absence of sensory dysfunction may not be detected by an OAE test.

OAE and ABR tests are recommended for identifying infants at risk for hearing impairment in the birth-admission screening (Norton *et al.*, 2000). According to the JCIH, infants who do not pass a birth-admission screening should be rescreened within 1 month of hospital discharge, and those infants who do not pass the rescreening should receive a comprehensive audiological evaluation by age 3 months. The overall goal is that infants with confirmed hearing loss receive a medically appropriate intervention by age 6 months.

The birth-admission screening exam recommended by JCIH does not include middle-ear or acoustic-reflex testing. The audiological assessment in the one-month rescreening exam (up to 6 months) includes 1000-Hz admittance tympanometry, but acoustic reflex testing is not recommended until age 6 months. These recommendations were based on earlier research that found difficulties in interpreting single-frequency admittance tympanograms in newborns and that many infants with normal hearing had an absent acoustic-reflex response.

Intrinsic limitations of NHS testing include the problem of false positives, i.e., those infants with normal hearing that are referred as impaired on the NHS exam, and false negatives, those infants later found to have a permanent hearing loss who pass the NHS exam as having normal function. The positive predictive value, which is the proportion of infants referring on the exam who are later confirmed to have a permanent hearing loss, of the NHS rescreening exam is only 6.7% (Thompson *et al.*, 2001), and even less in the initial birth-admission screening. That is, most infants referred by NHS do not have a hearing loss. The most common reason for referring on NHS exams is a transient middle-ear dysfunction that is present at the time of testing but that resolves thereafter. The presence of middle-ear dysfunction increases the likelihood of an absent response on an OAE or ABR test irrespective of whether the infant has normal hearing or a hearing loss. The problem of false positives, which number in the post-rescreening exam period in the many tens of thousands of infants every year in the U.S., increases screening and rescreening costs, generates anxiety in parents, lessens confidence in early hearing detection programs, and delays the discovery of the true hearing status.

A promising recent development in research is the fact that wideband tests of middle-ear function are feasible in newborns and can account for about 80% of the false-positives in a birth-admission NHS exam using OAEs (Keefe *et al.*, 2003). Wideband absorbance was more accurate than 1000-Hz admittance tympanometry in classifying OAE outcomes (as pass or refer) from NHS (Sanford *et al.*, 2009; Hunter *et al.*, 2010). In one- and two-day-old infants, an acoustic-reflex threshold was present in 97% of ears that passed the NHS exam (Keefe *et al.*, 2010). A combination of wideband absorbance and reflex testing performed better than either test alone in predicting the outcome of the NHS exam. As described above, ABR testing is recommended in the birth-admission screening test for infants in a NICU because of its ability to detect auditory neuropathy/dyssynchrony. It is of interest that an elevated or absent acoustic reflex test detected auditory neuropathy/dyssynchrony in 100% of adult test ears (Berlin *et al.*, 2005). This finding suggests the hypothesis, as yet untested, that wideband reflex testing may also detect this disorder in infant ears. The results to date lend confidence that more extensive combinations of acoustical tests of middle-ear, cochlear and neural function may be beneficial for screening and diagnosing hearing loss in infants. This is an active area of current research that may improve programs dedicated to early hearing detection and intervention. AT

Acknowledgments

Research described in this article has been funded for more than two decades by grants from the National Institute on Deafness and Communication Disorders. The author is grateful for his many constructive interactions with research colleagues during this time. Walt Jesteadt provided helpful comments on this article.

References

Abdala, C. (**2001**). "Maturation of the human cochlear amplifier: Distortion product otoacoustic emission suppression tuning curves recorded at low and high primary tone levels," J. Acoust. Soc. Am. **110**, 1465–1476.

Abdala, C., and Keefe, D. H. (**2012**). "Development of the ear: morphology and function," in *Human Auditory Development*, edited by L. Werner, A. N. Popper, and R. R. Fay, Springer Handbook of Auditory Research 42 (Springer, New York), Chap. 2, pp. 19–59.

von Békésy, G. (**1989**). *Experiments in Hearing*, translator and editor, Wever, E. G. (Acoustical Society of America, New York). This book was originally published in 1960.

Berlin, C. I., Hood, L. J., Morlet, T., Wilensky, D., St. John, P., Montgomery, E., and Thibodaux, M. (**2005**). "Absent or elevated middle ear muscle reflexes in the presence of normal otoacoustic emissions: A universal finding in 136 cases of auditory neuropathy/dyssynchrony," J. Am. Acad. Audiol. **16**, 546–553.

Brass, D., and Kemp, D. T. (**1993**). "Suppression of stimulus frequency otoacoustic emissions," J. Acoust. Soc. Am. **93**, 920–939.

Brown, A.M., and Kemp, D. T. (**1984**). "Suppressibility of the 2f1-f2 stimulated acoustic emissions in gerbil and man," Hearing Res. **13**, 29–37.

Don, M., and Kwong, B. (**2009**). "Auditory brainstem response: Differential diagnosis," in *Handbook of Clinical Audiology*, Sixth Edition, edited by J. Katz, L. Medwetsky, R. Burkhard, and L. Hood (Wolters Kluwer, Philadelphia), Chap. 13, pp. 265–292.

Feeney, M. P., and Keefe, D. H. (**1999**). "Acoustic reflex detection using wide-band acoustic reflectance, admittance, and power measurements," J. Speech, Language, and Hearing Res. **42**, 1029–1041.

Goldstein, J. L. (**1967**). "Auditory nonlinearity," J. Acoust. Soc. Am. **41**, 676–689.

Goldstein, J. L., and Kiang, N. Y.-S. (**1968**). "Neural correlates of the aural combination tone 2f1-f2," Proceed. Inst. Electrical and Electronics Engineers **56**, 981–992.

Gorga, M. P., Neely, S. T., Kopun, J., and Tan, H. (**2011**). "Distortion-product otoacoustic emission suppression tuning curves in humans," J. Acoust. Soc. Am. **129**, 817–827.

Holte, L., Margolis, R. H., and Cavanaugh, R. M. (**1991**).

"Developmental changes in multifrequency tympanograms," Intl. J. Audiol. **30**, 1–24.

Hudde, H. (**1983**). "Measurement of eardrum impedance of human ears," J. Acoust. Soc. Am. **73**, 242–247.

Hunter, L. L., Feeney, M. P., Miller, J. A. L., Jeng, P. S., and Bohning, S. (**2010**). "Wideband reflectance in newborns: Normative regions and relationship to hearing-screening results," Ear and Hearing **31**, 599–610.

Hunter, L., Ries, D. T., Schlauch, R. S., Levine, S. C., and Ward, W. D. (**1999**). "Safety and clinical performance of acoustic reflex tests," Ear and Hearing **20**, 506–514.

Joint Committee on Infant Hearing (**2007**). "Year 2007 position statement: Principles and guidelines for early hearing detection and intervention programs," Pediatrics **120**, 898.

Keefe, D. H., and Abdala, C. (**2007**). "Theory of forward and reverse middle-ear transmission applied to otoacoustic emissions in infant and adult ears," J. Acoust. Soc. Am. **121**, 978–993.

Keefe, D. H., and Abdala, C. (**2011**). "Distortion-product otoacoustic-emission suppression tuning in human infants and adults using absorbed sound power," J. Acoust. Soc. Am. **129**, EL108–113.

Keefe, D. H., Bulen, J. C., Arehart, K. H., and Burns, E. M. (**1993**). "Ear-canal impedance and reflection coefficient in human infants and adults," J. Acoust. Soc. Am. **94**, 2617–2638.

Keefe, D. H., Bulen, J. C., Campbell, S., and Burns, E. M. (**1994**). "Pressure transfer function and absorption cross-section from the diffuse field to the human infant ear canal," J. Acoust. Soc. Am. **95**, 355–371.

Keefe, D. H., Ellison, J. C., Fitzpatrick, D. F., and Gorga, M. P. (**2008**). "Two-tone suppression of stimulus frequency otoacoustic emissions," J. Acoust. Soc. Am. **123**, 1479–1494.

Keefe, D. H., Fitzpatrick, D. F., Liu, Y.-W., Sanford, C. A., and Gorga, M. P. (**2010**). "Wideband acoustic reflex test in a test battery to predict middle-ear dysfunction," Hearing Res. **263**, 52–65.

Keefe, D. H., Gorga, M. P., Neely, S. T., Zhao, F., and Vohr, B. R. (**2003**). "Ear-canal acoustic admittance and reflectance measurements in human neonates. II. Predictions of middle-ear dysfunction and sensorineural hearing loss," J. Acoust. Soc. Am. **113**, 407–422.

Keefe, D. H., and Levi, E. (**1996**). "Maturation of the middle and external ears: Acoustic power-based responses and reflectance tympanometry," Ear and Hearing **17**, 361–373.

Keefe, D. H., and Schairer, K. S. (**2011**). "Specification of absorbed-sound power in the ear canal," J. Acoust. Soc. Am. **129**, 779–791.

Kemp, D. T. (**1978**). "Stimulated acoustic emissions from within the human auditory system," J. Acoust. Soc. Am. **64**, 1386–1391.

Kemp, D. T. (**1979a**). "The evoked cochlear mechanical response and auditory microstructure—Evidence for a new element in cochlear mechanics," Scandinavian Audiology Supplement **9**, 35–47.

Kemp, D. T. (**1979b**). "Evidence of mechanical nonlinearity and frequency selective wave amplification in the cochlea," Archives of Otorhinolaryngol. **224**, 37–45.

Kiang, N. Y. S., Watanabe, T., Thomas, E. C., and Clark, L. F. (**1965**). *Discharge Patterns of Single Fibers in the Cat's Auditory Nerve* (MIT Press, Cambridge).

Liu, Y.-W., Sanford, C. A., Ellison, J. C., Fitzpatrick, D. F., Gorga, M. P., and Keefe, D. H. (**2008**). "Wideband absorbance tympanometry using pressure sweeps: System development and results on adults with normal hearing," J. Acoust. Soc. Am. **124**, 3708–3719.

Metz, O. (**1946**). "The acoustic impedance measured on normal and pathological ears," Acta Oto-laryngologica (Stockholm), supplement **63**, 1–245.

Nomoto, M., Suga, N., and Katsuki, Y. (**1964**). "Discharge pattern and inhibition of primary auditory nerve fibers in the monkey," J. Neurophysiol. **27**, 768–787.

Norton, S. J., Gorga, M. P., Widen, J. E., Folsom, R. C., Sininger, Y., Cone-Wesson, B., Vohr, B. R., and Fletcher, K. (**2000**). "Identification of neonatal hearing impairment: Summary and recommendations," Ear and Hearing **21**, 529–535.

Nuttall, A. L., Dolan, D. F., and Avinash, G. (**1990**). "Measurements of basilar membrane tuning and distortion with laser Doppler velocimetry," in *The Mechanics and Biophysics of Hearing, edited* by P. Dallos, C. D. Geisler, J. W. Matthews, M. A. Ruggero, and C. R. Steele (Springer-Verlag, Berlin), pp. 288–295.

Qi, L., Liu, H., Lutfy, J., Funnell, W. R. J., and Daniel, S. J. (**2006**). "A nonlinear finite-element model of the newborn ear canal," J. Acoust. Soc. Am. **120**, 3789–3798.

Rhode, W. S. (**1971**). "Observations of the vibration of the basilar membrane in squirrel monkeys using the Mössbauer technique," J. Acoust. Soc. Am. **49**, 1218–1231.

Rhode, W. S. (**1977**). "Some observations of two-tone interactions measured using the Mössbauer effect," in *Psychophysics and Physiology of Hearing*, edited by E. F. Evans and J. P. Wilson (Academic Press, New York), pp. 27–38.

Robles, L., Ruggero, M. A., and Rich, N. C. (**1990**). "Two-tone distortion on the basilar membrane of the chinchilla cochlea," in *The Mechanics and Biophysics of Hearing*, edited by P. Dallos, C. D. Geisler, J. W. Matthews, M. A. Ruggero, and C. R. Steele (Springer-Verlag, Berlin), pp. 304–311.

Rosowski, J. J., Carney, L. H., and Peake, W. T. (**1988**). "The radiation impedance of the external ear of the cat: Measurements and applications," J. Acoust. Soc. Am. **84**, 1695–1708.

Sachs, M. B., and Kiang, N. S. (**1967**). "Two-tone inhibition in auditory-nerve fibers," J. Acoust. Soc. Am. **43**, 1120–1128.

Sanford, C. A., Keefe, D. H., Liu, Y.-W., Fitzpatrick, D. F., McCreery, R. W., Lewis, D. E., and Gorga, M. P. (**2009**). "Sound-conduction effects on distortion-product otoacoustic emission screening outcomes in newborn infants: Test performance of wideband acoustic transfer functions and 1-kHz tympanometry," Ear and Hearing **30**, 635–652.

Shanks, J. E., and Lilly, D. J. (**1981**). "An evaluation of tympanometric estimates of ear canal volume," J. Speech and Hearing Res. **24**, 557–566.

Shaw, E. A. G. (**1988**). "Diffuse-field response, receiver impedance, and the acoustical reciprocity principle," J. Acoust. Soc. Am. **84**, 2284–2287.

Shera, C. A., Guinan, J. J., Jr., and Oxenham, A. J. (**2010**). "Otoacoustic estimation of cochlear tuning: Validation in the chinchilla," J. Assn. Res. Otolaryngol. **11**, 343–365.

Stinson, M. R., Shaw, E. A. G., and Lawton, B. W. (**1982**). "Estimation of acoustical energy reflectance at the eardrum from measurements of pressure distribution in the human ear canal," J. Acoust. Soc. Am. **73**, 766–773.

Teranishi, R., and Shaw, E. A. G. (**1968**). "External-ear acoustic models with simple geometry," J. Acoust. Soc. Am. **44**, 257–263.

Terkildsen, K., and Thomsen, K. A. (**1959**). "The influence of pressure variations on the impedance of the human ear drum," J. Laryngol. & Otology **73**, 409–418.

Thompson, D. C., McPhillips, H., Davis, R. L., Lieu, T. A., Homer, C. J., and Helfand, J. (**2001**). "Universal newborn hearing screening: Summary of evidence," J. Am. Med . Assn. **286**, 2000–2010.

Voss, S., and Allen, J. B. (**1994**). "Measurement of acoustic impedance and reflectance in the human ear canal," J. Acoust. Soc. Am. **95**, 273–384.

Douglas H. Keefe received an A.B. degree in Psychology from the University of Michigan, and M.S. and Ph.D. degrees in Physics from Illinois Institute of Technology and Case Western Reserve University, respectively. After work on acoustics and vibration consulting and research on respiratory physiology, Doug performed musical acoustics and hearing research at the University of Washington. He is a Senior Research Scientist at Boys Town National Research Hospital, where he has worked in the Center for Hearing Research since 1995. His research concerns basic and translational clinical research on middle-ear and cochlear function. Technology transferred from research contributes to commercial development of new hearing screening and diagnostic devices. He is a Fellow of the Acoustical Society of America and has chaired its Technical Committee on Musical Acoustics.